BAB V
PENUTUP

V.1 Spesifikasi

Pompa sentrifugal untuk memompa air :

Kapasitas pompa	:	10300 m^3/jam
Tekanan maximum	:	30 m.k.a
Kecepatan pompa	:	253 rpm

Dari hasil perhitungan diperoleh :

Daya penggerak pompa	:	1502,08 dk
Diameter poros pompa	:	26 cm
Jumlah sudu	:	9 buah

Ukuran – ukuran impeller disisi masuk :

Diameter inlet dam	:	130 cm
Lebarsudu	:	37,7 cm
Sudut masuk absolut	:	90°
Lengkungan sudu	:	10°

Ukuran – ukuran impeller disisi keluar :

Diameter outlet impeller	:	208 cm
Lebar sudu	:	24,6 cm
Sudut keluar absolut	:	127°
Lengkungan sudu	:	26°

Ukuran – ukuran pokok pompa :

Panjang pompa	:	310 cm
Tinggi pompa	:	264 cm
Lebarpompa	:	237 cm

V.2 Kesimpulan

Karena pompa yang direncanakan adalah untuk memompa air laut. Sehingga bahan dari bagian-bagian pompa harus dibuat dari bahan yang mempunyai ketahanan yang baik terhadap korosi oleh air laut.

a. Poros pompa

Air laut yang sifatnya korrosive terhadap besi/baja, sehingga poros pompa dibuat dari baja tahan karat (stainless steel) dengan tegangan-tegangan yang diijinkan.

b. Impeller

Impeller dibuat dari bahan Bronze, dengan cara dicor. Permukaan dari impeller terutama bagian yang dilalui aliran air, dibuat sehalus mungkin untuk memperbesar effisiensi pompa. Setelah selesai dan dipasang pada poros, impeller harus dibalans secara statis maupun dinamis untuk menghindari getaran yang timbul pada waktu pompa bekerja.

c. Rumah pompa (casing)

Untuk tekanan yang rendah rumah pompa (casing) dibuat dari besi tuang. Besi tuang lebih tahan terhadap korosi dibanding dengan besi atau baja. Disinipun permukaan yang dilalui aliran air harus dibuat halus untuk memperoleh effisiensi yang maksimal. Stuffing box dibuat pada casing untuk memperoleh kerapatan yang baik antara poros dan casing. Didalamnya diisi dengan packing yang lunak, kemudian ditekan oleh penekan packing yang dibuat dari besi tuang baja. Dipasaran packing yang dibuat dari bahan katun atau hennep dibuat dengan penampang potongan segi empat dan digulung menurut bentuk koil yang bisa dipotong-potong menurut kebutuhan. Dipasaran packing tersebut sering disebut Reimers Packing.

d. Pasak (key)

Seperti halnya poros pompa, pasak dibuat dari besi tahan karat (stainless steel), dengan kekuatan bahan seperti yang telah dipakai dalam perhitungan. Pasak untuk kopling pompa bisa dibuat dari bahan besi biasa karena bekerja tanpa dipengaruhi oleh bahan yang korrosive.

e. Kopling pompa

Kopling ini bekerja tanpa dipengaruhi oleh bahan yang korrosive sehingga bisa dibuat dari bahan besi/baja biasa dengan kekuatan bahan seperti yang telah dipakai dalam perhitungan. kopling elastis mempergunakan bahan kulit yang dipasang pada baut-baut kopling.

f. Ballbearing

Karena ballbearing dibuat oleh pabrik tertentu dan dipasaran tersedia sebagai bagian (parts) mesin yang siap untuk dipakai, maka mengenai bahan ini tidak akan diuraikan disini. Pelumasan yang baik perlu untuk mendapatkan umur bearing yang maximal. pelumasan direncanakan mempergunakan minyak pelumas.

DAFTARNOTASI

Tabulasi berikut menunjukkan simbol yang digunakan pada tugas perancangan ini. Karena huruf terbatas, kadangkala huruf yang sama digunakan untuk menyatakan lebih dari satu konsep.

A	=	Luas penampang aliran	→	cm^2
B	=	Lebar	→	cm
b	=	Lebar	→	cm
C	=	Kecepatan absolute	→	m/sec
D	=	Diameter	→	cm
d	=	Diameter	→	cm
F	=	Luas penampang bahan	→	cm^2
H	=	Total head	→	mka
h	=	Suction/ delivery head	→	m
Ka	=	Gaya aksial	→	kg
L	=	Panjang	→	cm
M	=	Moment	→	kg.cm
N	=	Daya	→	d.k / p.k
n	=	Putaran	→	rpm
n_s	=	Putaran spesifik	→	–
P	=	Gaya	→	kg
Q	=	Kapasitas pompa	→	m^3/h, gpm
R	=	Radius	→	cm
S	=	Tebal	→	cm
t	=	Jarak	→	cm
U	=	Kecepatan tangensial	→	m/sec
V	=	Kecepatan aliran	→	m/sec
w	=	Moment tahanan	→	cm^3
W	=	Kecepatan aliran relatif	→	m/sec

X	=	Beda antara 2 radius	→	cm
Z	=	Jumlah sudu	→	–
α	=	Sudut absolut	→	derajat
β	=	Sudut lengkungan sudu	→	derajat
γ	=	Density air	→	kg/dm^3
ε	=	Faktor pemasukan	→	–
Φ	=	Head coefficient	→	–
Ø	=	Sudut	→	derajat
ρ	=	Tangent circular arcs	→	cm
η_p	=	Effisiensi pompa	→	–
$\eta_{\sim}$	=	Coeffisient of circulatory flow	→	–
θ	=	Sudut	→	derajat
Б_b	=	Teganganlengkung	→	kg/cm^2
Б_d	=	Tegangan tekan	→	kg/cm^2
Б_{dr}	=	Tegangan tekan bidang	→	kg/cm^2
τ_w	=	Tegangan puntir	→	kg/cm^2
τ_D	=	Tegangan geser	→	kg/cm^2

DAFTAR PUSTAKA

1. CENTRIFUGAL PUMPS AND BLOWER.

   Karangan : Austin H. Church.

   Penerbit : John Wiley & Sons, Inc.

   New York, London.

   Edisi : 8 th printing, March 1960.

2. POMPA.

   Karangan : Ir. L.W.P. Bianchi.

   P. Bustraan.

   Alihbasa : Hendardji.

   Penerbit : Penerbit Buku Tehnik H. STAM Jakarta.

   Edisi : Cetakan ke 2,1953.

3. KENT'S MECHANICAL ENGINEERS' HANDBOOK.

   DESIGN AND PRODUCTION VOLUTE.

   Karangan : Colin Carmichael.

   Penerbit : John Wiley & Sons, Inc, New York.

   Mei Ya Publications, Inc, Taipei.

   Edisi : 12th edition, 1973.

4. MARINE AUXILIARY MACHINERY AND SYSTEMS.

   Karangan : M. Khetagurov.

   Penerbit : Peace Publisher Moscow.

   Edisi : –

5. UNIT OPERATIONS OF CHEMICAL ENGINEERING.

Karangan	:	Warren L. Mc Cabe.
		Julian C. Smith.
Penerbit	:	Mc Graw Hill Kogakusha, Ltd.
		Tokyo, Japan.
Edisi	:	1976.

6. POMPA.

Karangan	:	Ing. A. Nouwen.
Penerbit	:	Bhratara – Jakarta
Edisi	:	1981.

7. PUMP HANDBOOK.

Karangan	:	Igor J. Karassik, William C. Krutzsch,
		Warren H Fraser, Josep P. Messina
Penerbit	:	New York
Edisi	:	1957.

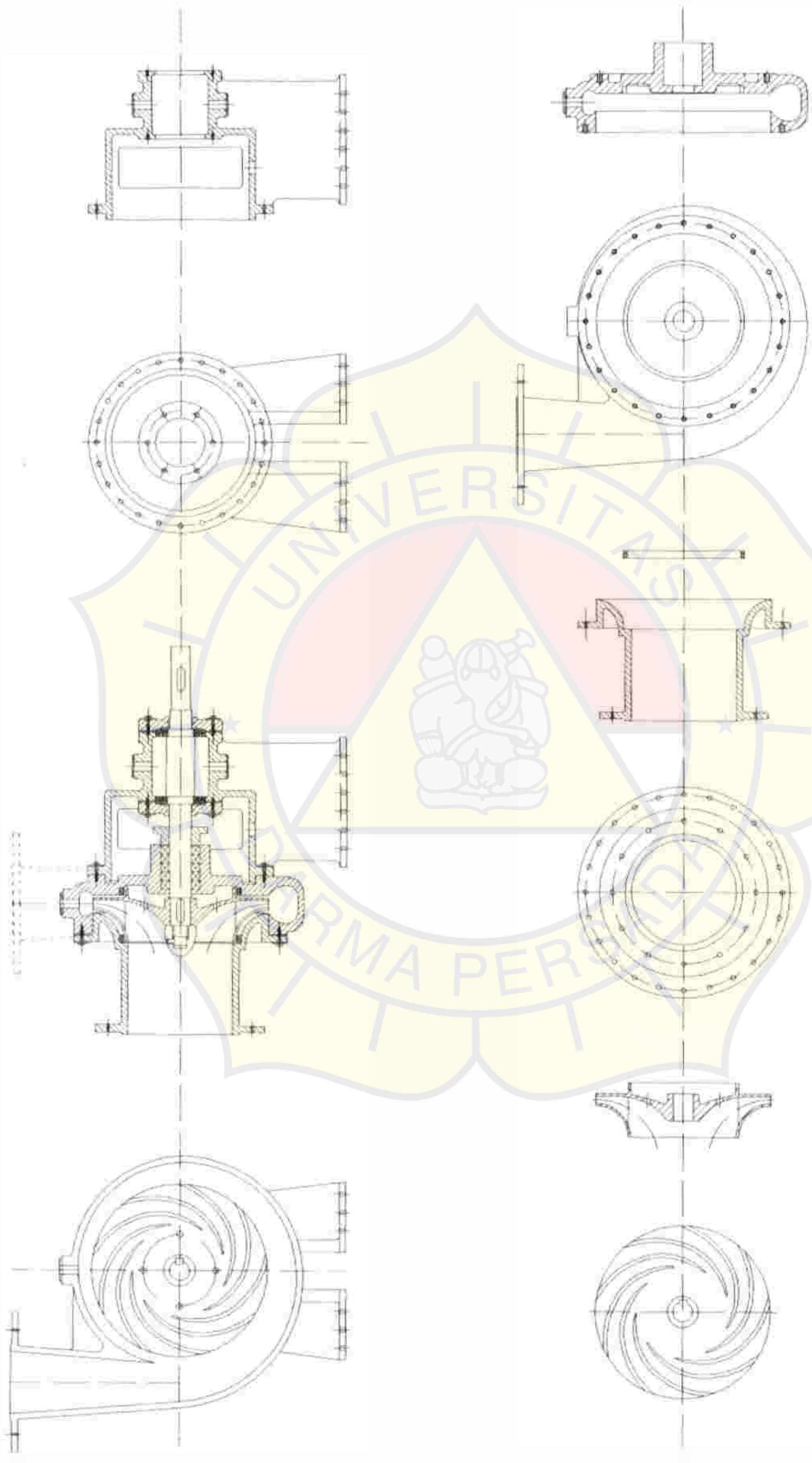

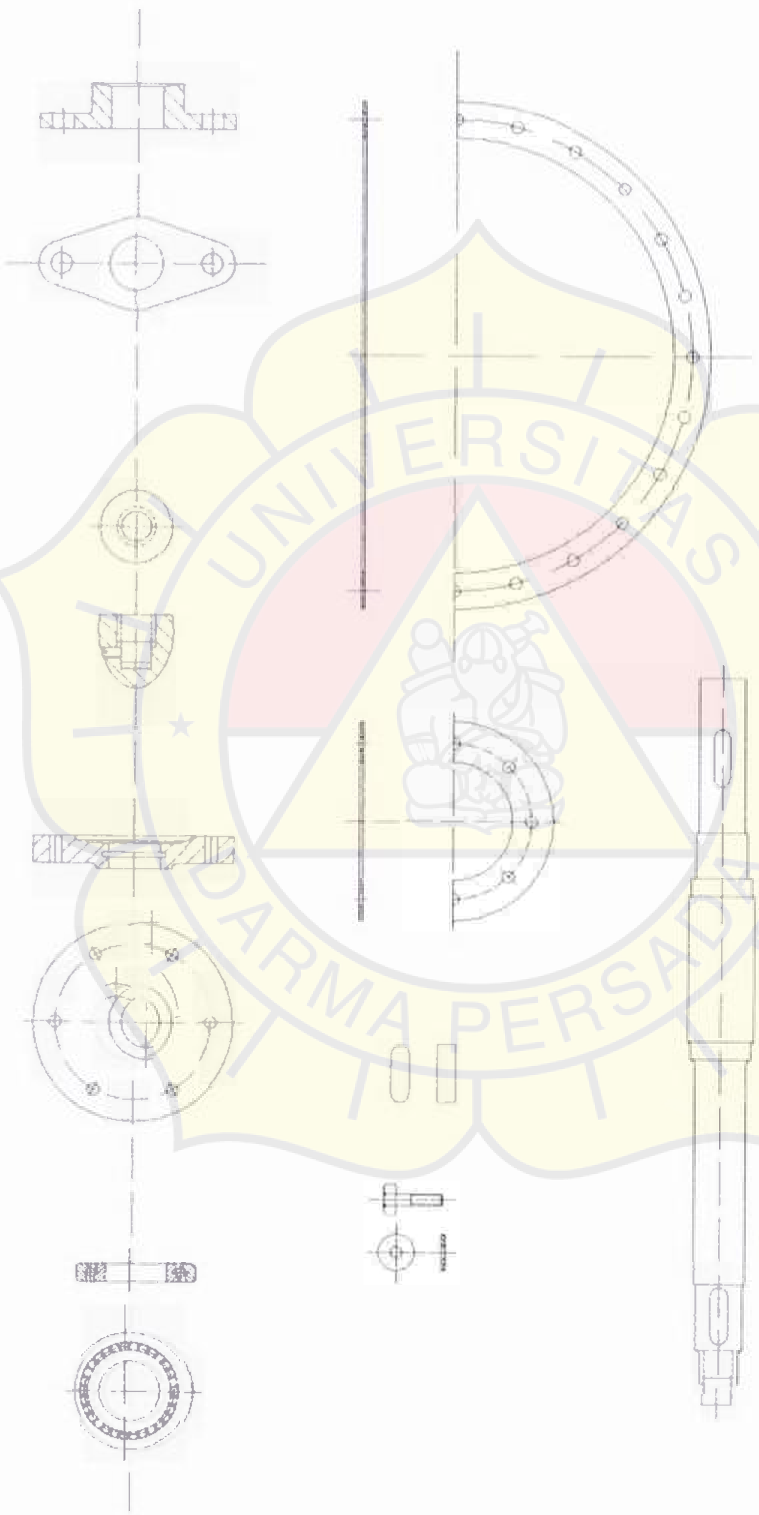

The efficiency of pumps falls off very rapidly for specific speeds less than about 20, because low specific speed impellers have long narrow vane passages which result in large fluid friction losses and greater disc friction losses. In addition, the amount of leakage is

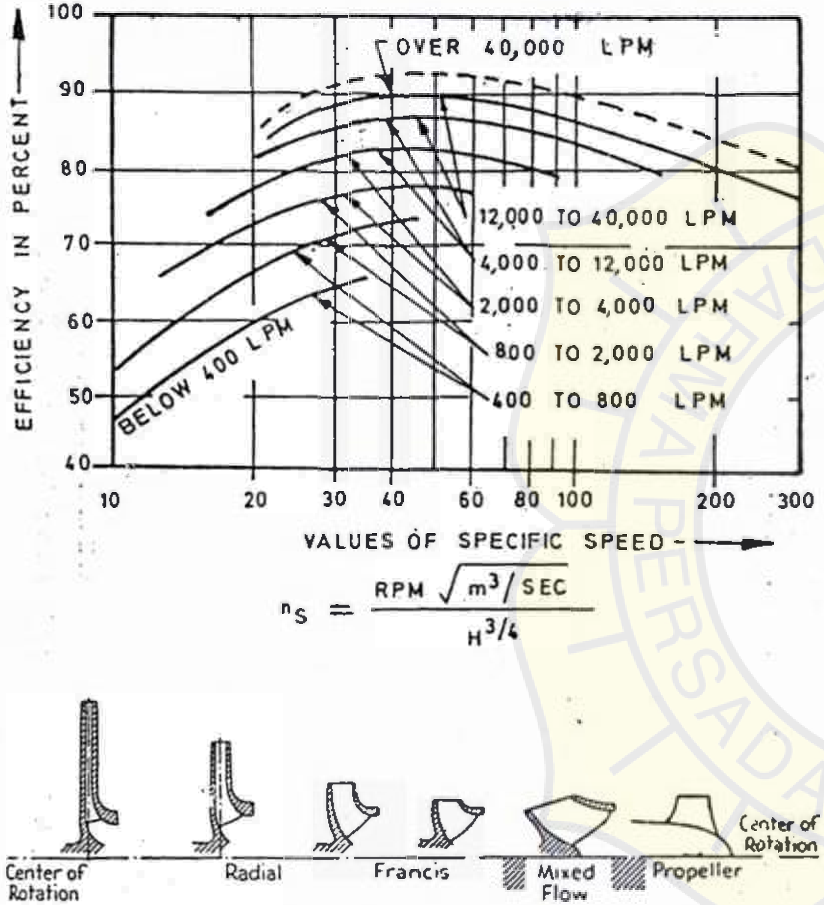

Courtesy Worthington Pump & Machinery Corp.

Fig 4.18 Approximate relative impeller shapes and efficiencies as related to specific speed.

proportionally greater as the leakage area is a greater percentage of the passage area for small flows and the pressure differential is greater.

impeller and hence a smaller and cheaper pump. In general the efficiency will also be higher.

In Figs 4.15, 4.16 and 4.17 the capacity of the double-suction stages is taken as one-half the pump capacity, i.e., the plotted points are reduced to the equivalent of single-suction impellers, as explained in Section 4.3. The pumps include both single- and multistage machines and, although the efficiency of the multistage units is generally slightly lower than the single-stage, the difference is neither very great nor consistent.

4.6 Model Tests—It is desirable to be able to predict the efficiency to be expected from large pumps on the basis of tests made on smaller homologous pumps. In designing large pumps, as for water supply systems, tests are sometimes made on models with the aim of securing the best design. If the larger pump or prototype is homologous with the model and if the two have the same proportionate degree of surface roughness, it has been found that the prototype will have a slightly higher efficiency than the model.

The same problem is met in hydraulic turbine design. Various formulas have been developed in this field, and these are applied to pumps. One of the earlier equations developed was the Camerer formula :

$$E=1-(1-e)\frac{0{\cdot}12+\dfrac{0{\cdot}024}{\sqrt{(A_2/U_2D)D}}}{0{\cdot}12+\dfrac{0{\cdot}024}{\sqrt{(A_2/U_2D)d}}} \qquad \dots (4.3)$$

where e is the efficiency of the model ;
E is the efficiency of the prototype ;
d is the runner diameter of the model ;
D is the runner diameter of the prototype ;
A_2/U_2D is the ratio of the outflow area, A_2, of the runner to the product of the wetted perimeter and the runner diameter, i.e., the ratio of the hydraulic radius of the exit area to the runner diameter.

This equation is complicated; it requires a knowledge of the dimensions of the impeller to get the hydraulic radius ; and in addition the co-efficients change with the wheel type. Moreover it is based upon friction losses alone, neglecting turbulence.

or

$$D_0 = \sqrt{\frac{4}{\pi} \frac{Q}{v_0} + D^2_H} \qquad \text{... (6.1)}$$

The leakage loss usually ranges between 2 and 10 per cent of the delivered flow Q. Hence in applying Eqn 6.1 the total flow Q should be increased by this amount. After the outlet diameter of the impeller has been fixed, the leakage flow may be estimated according to Section 6.4.

The inlet vane edge diameter D_1 is usually made about the same as the eye diameter D_0 to insure smooth flow without excessive turbulence. If the inlet edge of the vane is sloped as shown in Fig 6.2 an average value is used for D_1.

Since slowing up a fluid is always more inefficient than speeding it up, the radial inlet velocity at the vane inlet v_{r_1} is usually made 5 to 10 per cent greater than v_0. These assumed values of v_{r_1} and D_1 determine the width of the impeller at the inlet, b_1. By the continuity equation

$$b_1 = \frac{Q}{\pi D_1 v_{r_1} \varepsilon_1} \text{ in m.} \qquad \text{...(6.2)}$$

The gross inlet area $\pi D_1 b_1$ is not available to the fluid, but is reduced by the vane thickness. This is accounted for by assuming a contraction factor ε_1 which is generally between 0·8 and 0·9, in the preliminary calculation of the impeller inlet width b_1. After the number of vanes and their inlet thickness have been determined, the exact value of the coefficient ε_1 may be found and, if necessary, the inlet width is corrected to give the required area.

The water is usually assumed to enter the vanes radially as discussed in Chapter 3, so that the absolute approach angle α_1 is 90°. Having determined v_{r_1} and u_1, the vane inlet angle β_1 is found from

$$\tan \beta_1 = \frac{v_{r_1}}{u_1} \qquad \text{...(6.3)}$$

This value of $\tan \beta_1$ is usually increased slightly to care for the contraction of the stream as it passes the inlet edges and the prerotation of the water (Section 3.8). It is increased more for high suction lifts and small ratios of D_2/D_1 (i.e., higher specific speed impellers). The inlet angle usually falls in the range from 10° to 25°.

Guide vanes could be placed before the impeller to give v_{u_1} a negative value and thus raise the head and overall efficiency at the design condition, but the head and efficiency would drop off more rapidly at partial capacities.

6.6 Flow in Impellers—Before proceeding with the impeller design it is important to consider the flow conditions existing in the fluid passage and at the impeller outlet.

The effect of the circulatory flow has already been discussed in Section 3.6. As noted there, the magnitude of this effect is very difficult to determine. Various experiments have been performed to determine the flow conditions existing in the impeller.

Fischer and Thoma[1] used an impeller having six vanes cast integral with the front shroud and a circular glass plate for a back shroud. They injected a dark-coloured dye into the water and observed the flow by means of a "rotoscope" and camera. They found that the flow conditions, especially at low discharges, were entirely different from the ideal assumptions. The water passages were never completely filled with active flow, and the flow broke away from the vane surfaces. Dead water volumes formed in the passages on the low pressure side of the vanes. When the delivery was below the design point, the outward flow was no longer stable. The fluid in some instances even came out of the inlet of one passage and went into the next passage. At shut-off, instead

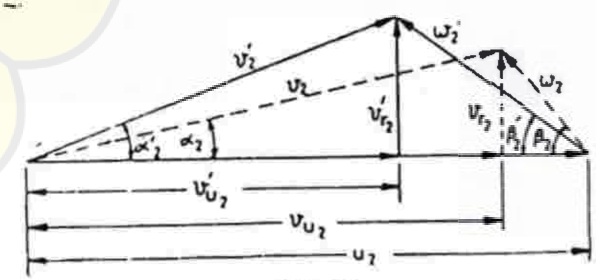

Fig 6.3

of having one vortex for the impeller, there was a series of small vortices which resulted from the fluid friction. These conditions

* Throughout this chapter Q will have the units of cubic metres per second.

1 K. Fischer and D. Thoma, "Investigation of the Flow Conditions in a Centrifugal Pump," *A.S.M.E. Trans.*, HYD-54-8, 1932.

undoubtedly account for the curious breaks occurring in the head-capacity curves obtained on extremely accurate laboratory tests (see Figs 3.24 and 3.25). As the result of careful measurements with a pitot tube T. Kasai,[1] R. C. Binder and R. T. Knapp[2] found similar conditions existed.

Since the passages may not be completely filled with active flow, the radial outlet velocity v_{r_2} may be greater than the calculated value. Hence, the actual outlet diagram will appear as shown in solid lines in Fig 6.3. For comparison the ideal diagram uncorrected for circulatory flow is shown in dashed lines. As may be seen from the figure, the increase in the radial component of the absolute outlet velocity v_{r_2} decreases the absolute velocity v'_2 at which the liquid leaves the impeller and also increases the absolute outlet angle α'_2. There are not sufficient data available to calculate the magnitude of this change on the outlet diagram.

6.7 Impeller Outlet Dimensions and Vane Angle—By Eqn 3.37 the virtual head $H_{vir\infty}$ is

$$H_{vir\infty} = \frac{1}{g}\left[u_2^2 - \frac{u_2 v_{r_2}}{\tan\beta_2}\right]$$

and by Eqn 3.25 the total head H is

$$H = K\frac{u_2 v_{u_2}}{g} = KH_{vir\infty}$$

Combining these equations

$$\frac{Hg}{K} = u_2^2 - \frac{u_2 v_{r_2}}{\tan\beta_2}$$

or

$$u_2^2 - \frac{v_{r_2}}{\tan\beta_2}u_2 - \frac{Hg}{K} = 0$$

which is a quadratic equation in u_2. Solving this for u_2,

$$u_2 = \frac{1}{2}\left[\frac{v_{r_2}}{\tan\beta_2} + \sqrt{\left(\frac{v_{r_2}}{\tan\beta_2}\right)^2 + \frac{4gH}{K}}\right]$$

Since $K = \eta_\infty \eta_{HY}$ this equation shows the effect of the various factors on u_2. For radial-type impellers η_∞ varies between 0·65 and 0·75, and K varies between 0·6 and 0·7, the larger value applying to lower specific speed impellers.

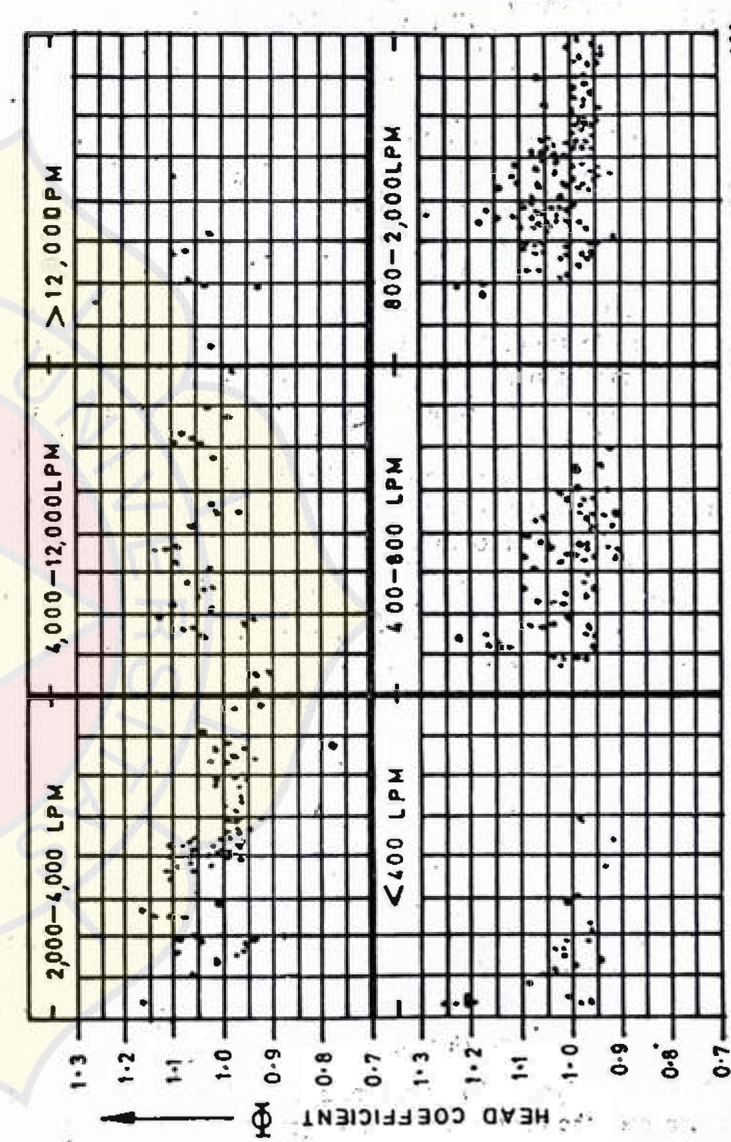

Fig 6.4 Head coefficient ϕ *versus* head points for various *capacity* ranges.

[1] T. Kasai, "On the Exit Velocity and Slip Coefficient of Flow at the Outlet of the Centrifugal Pump Impeller," *Memoirs of Faculty of Engineering*, Kyushu Imperial University, 1926, Vol. 8, No. 1, pp. 1-89.

[2] R. C. Binder and R. T. Knapp, "Experimental Determinations of the Flow Characteristics in the Volutes of Centrifugal Pumps," *A.S.M.E. Trans.*, HYD-58-4, 1936.

... can be more easily obtained by means of the overall head coefficient ϕ as developed in Section 3.14(*d*). By Eqn 3.27, $D_2 = \frac{84 \cdot 5\phi\sqrt{H}}{n}$. The value of ϕ varies between 0·9 and 1·20 with an average value very close to unity. Since it varies with the outlet angle and impeller dimensions, there will be a range of values for any given head, capacity, or specific speed. Figures 6.4, 6.5, and 6.6 show plots of ϕ against these factors for the group of pumps cited in Section 4.5. These figures may be used to select a value of ϕ for given operating conditions.

The outlet vane angle β_2 may be selected within fairly wide limits. The relationship between it and the characteristic curve was discussed in Section 3.16. In general, backward-curved vanes are used for pump impellers since, as illustrated in Fig 3.21, the portion of the total head which is in the form of velocity is a minimum for backward-curved vanes. Because the velocity head is difficult to convert into pressure head efficiently, impellers having radial or forward-curved vanes are less efficient than the backward-curved type. Moreover, radial or forward-curved vanes have an undesirable passage shape between the vanes which is difficult for the liquid to follow; this results in eddy losses. The angle β_2 is usually made between 15° and 40°. It is usually made slightly larger than the inlet angle to obtain a smooth, continuous passage.

The radial outlet velocity v_{r_2} is ordinarily made equal to or slightly less (up to 15 per cent) than the radial inlet velocity v_{r_1} to avoid any sudden changes of velocity.

A contraction factor ε_2, to compensate for the vane thickness at the outlet, is assumed subject to correction after the actual thickness and the number of vanes have been determined. This factor ε_2 is usually between 0·90 and 0·95. The approximate outlet width is then found from

$$b_2 = \frac{Q}{v_{r_2} D_2 \pi \varepsilon_2} \text{ in metres} \qquad \ldots(6.4)$$

6.8 Design of Vanes—The vane angles and diameters having been determined, the next step in the design of the stage is to construct the vane shape. There is no published information concerning the effect of the vane curvature between the inlet and exit on the pump efficiency, although it must have a great influence. The passage should not be too long because this would

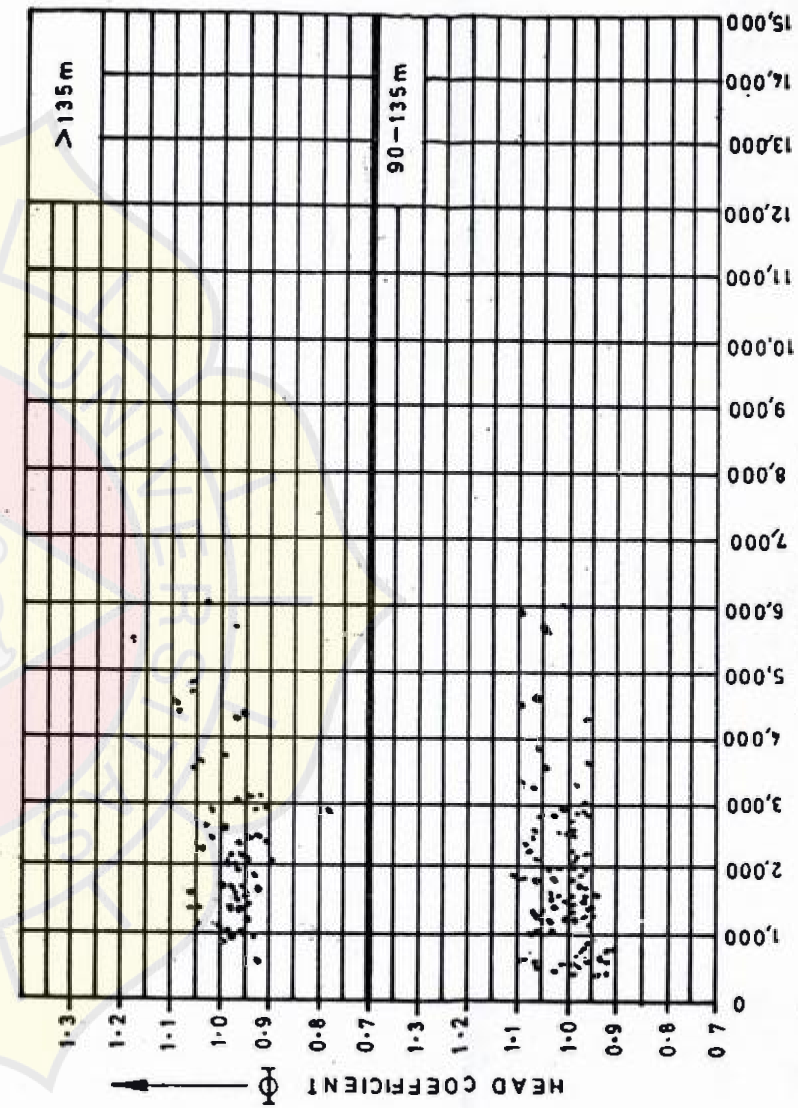

Fig 6.5(a) Head coefficient ϕ *versus* capacity points for various *head* ranges.

motion. Owing to the increased turbulence when the angles are not in agreement, the efficiency drops off rapidly. For rounded inlet edges, the efficiency does not reach the peak value of the sharp edge vane, but neither does it drop off as rapidly for incorrect angles.

The number of vanes z is based largely upon experience and is fixed after the vane shape has been determined. There should be enough vanes to secure proper guidance of the liquid. Too many vanes will result in excessive friction losses. A general rule is to make the cross section of the passage approximately square, as this will reduce the frictional resistance to a minimum. Pfleiderer, in *Die Kreiselpumpen*, gives the following equation for the number of vanes :

$$z = 6{\cdot}5\, \frac{D_2 + D_1}{D_2 - D_1} \sin \beta_m \qquad \ldots(6.7)$$

where $\beta_m = \dfrac{\beta_1 + \beta_2}{2}$. As may be noted from Pfleiderer's equation, large vane angles require more vanes in order to provide proper guidance to the liquid. The number of vanes generally used is between 5 and 12.

After the vane thickness and number of vanes have been decided upon, the contraction of the flow at any point due to the vanes may be found by

$$\varepsilon = \frac{\pi D - \dfrac{zt}{\sin \beta}}{\pi D} \qquad \ldots(6.8)$$

where ε is the contraction factor, z the number of vanes, and t the normal vane thickness.

The width of the impeller passage b at any point may then be calculated from

$$\text{Area } A = \pi D b \varepsilon = \frac{Q}{v_r} \text{ in square metres}$$

or

$$b = \frac{Q}{\pi D \varepsilon v_r} \text{ in metres} \qquad \ldots(6.9)$$

By means of Eqns 6.8 and 6.9 the values of ε and b at points along the impeller may be found including those at the inlet and discharge.

design procedure and to clarify the preceding sections, the design of an impeller for specified conditions will be considered. It should be kept in mind that the design will be greatly influenced in the interest of economy by previous impellers which have been made and for which the patterns are available. This factor must necessarily be neglected in the following example.

The pump will be designed to develop a head of 45 m and deliver 10 m³/min of water. It is to be direct-connected to a motor operating at 1760 rpm.

As 1 m³ of water weighs 1,000 kg the weight flow w is

$$w = \frac{10 \times 1000}{60} = 166{\cdot}7 \text{ kg/sec}$$

$$Q = \frac{10}{60} = 0{\cdot}167 \text{ m}^3/\text{sec}$$

Since water is practically incompressible, this volume of 0·167 m³/sec remains constant at all points in the pump.

A pump operating under the given conditions could be made single-suction, but in order to make the example more general a double-suction impeller will be used. This means that each side of the inlet will handle 5 m³/min and the impeller will discharge the total 10 m³/min at the periphery. The specific speed is

$$n_s = \frac{n\sqrt{Q}}{H^{3/4}} = \frac{1760 \times \sqrt{\dfrac{0{\cdot}167}{2}}}{45^{3/4}} = 29{\cdot}4$$

The water horsepower is

$$\text{whp} = \frac{wH}{75} = \frac{166{\cdot}7 \times 45}{75} = 100$$

From Fig 4.15 for a head of 45 m and 5 m³/min the overall efficiency will be between 75 and 88 per cent. From Fig 4.16 it will be between 72 and 87 per cent and from Fig. 4.17 for a specific speed of 29·4 the range is between 71 and 85 per cent. Probably 81 per cent would be a fair value to assume. The brake horsepower (from Eqn 3.30) is

$$\text{bhp} = \frac{\text{whp}}{\eta} = \frac{100}{0{\cdot}81} = 123{\cdot}5$$

The shaft torque is

$$T = \frac{715 \text{ bhp}}{n} = \frac{715 \times 123{\cdot}5}{1760} = 50{\cdot}2 \text{ kg-m}$$

A contraction factor ε_2 to care for the vane thickness must be assumed in determining the gross outlet area and width b_2. If this is tentatively taken to be 0·925, then by Eqn 6.4 the approximate outlet width is

$$b_2 = \frac{Q}{v_{r_2} \; \pi D_2 \varepsilon_2} = \frac{0{\cdot}167 \times 1{\cdot}02 \times 100}{3{\cdot}6 \times \pi \times 0{\cdot}354 \times 0{\cdot}925} = 4{\cdot}45 \text{ cm}$$

Outlet Velocity Diagram : To design correctly the volute or diffuser, the magnitude and direction of the absolute outlet velocity v_2 of the liquid leaving the impeller must be known. Sufficient data are now available to draw the outlet diagram.

For an outlet diameter D_2 of 35·4 cm and a speed of 1760 rpm the tip speed is

$$u_2 = \frac{\pi D_2 n}{60} = \frac{\pi \times 0{\cdot}354 \times 1760}{60} = 32{\cdot}6 \text{ m/sec}$$

The virtual tangential component v_{u_2} of the absolute outlet velocity v_2 is

$$v_{u_2} = u_2 - \frac{v_{r_2}}{\tan \beta_2} = 32{\cdot}6 - \frac{3{\cdot}6}{\tan 20°} = 22{\cdot}45 \text{ m/sec}$$

Assuming a value of $\eta_\infty = 0{\cdot}7$, the actual tangential component v'_{u_2} of the absolute outlet velocity v'_2 is, by Eqn 3.21,

$$v'_{u_2} = v_{u_2} \eta_\infty = 22{\cdot}45 \times 0{\cdot}7 = 15{\cdot}72 \text{ m/sec}$$

The outlet diagram may now be drawn (Fig 6.9). The tangent of the actual outlet angle α'_2 is $v_{r_2} / v'_{u_2} = \dfrac{3{\cdot}6}{15{\cdot}72} = 0{\cdot}228$ and $\alpha'_2 = 12{\cdot}8°$. On account of the actual flow conditions, described in

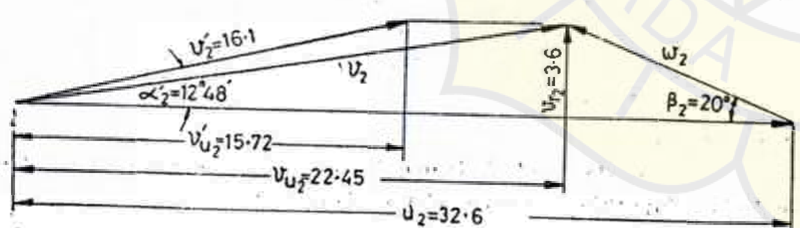

Fig 6.9 Outlet velocity diagram.

Section 6.6, this angle is probably slightly larger, say 13°. The absolute outlet velocity is

$$v'_2 = \sqrt{v_{r_2}^2 + v'^2_{u_2}} = \sqrt{3{\cdot}6^2 + 15{\cdot}72^2} = 16{\cdot}1 \text{ m/sec}$$

v_{r_2} will have a relatively minor effect, and v'_2 will probably not be less than 16·0 m/sec.

Leakage Loss : Sufficient data are now available to allow a closer approximation of the leakage in accordance with Section 6.4. From the impeller drawing (Fig 6.13) the mean diameter of the clearance D is 23 cm. The diametral clearance should be (Section 6.4)

$$s = 0{\cdot}25 + (D - 150) \times 0{\cdot}001 = 0{\cdot}25 + (230 - 150) \times 0{\cdot}001$$
$$= 0{\cdot}33 \text{ mm or } 0{\cdot}033 \text{ cm}$$

The clearance area

$$A = \frac{1}{2} \pi D s = \frac{1}{2} \pi \times 23 \times 0{\cdot}033 = 1{\cdot}20 \text{ cm}^2$$

The head across the rings will be

$$H_L = \frac{3}{4} \frac{u_2^2 - u_1^2}{2g} = \frac{3}{4} \left[\frac{32{\cdot}6^2 - 17{\cdot}5^2}{2 \times 9{\cdot}81} \right] = 28{\cdot}9 \text{ m}$$

If the wearing rings are plain, similar to No. 3 of Fig 6.1, the flow coefficient corresponding to a speed of 1760 rpm and a clearance of 0·32 mm will be 0·410. The leakage then will be

$$Q_L = C \cdot \frac{A}{10^4} \sqrt{2gH_L} = 0{\cdot}410 \times \frac{1{\cdot}2}{10^4} \times \sqrt{2 \times 9{\cdot}81 \times 28{\cdot}9} = 1{\cdot}18$$

$\times\ 10^{-3}$ m³/sec per side and the total leakage is $2{\cdot}36 \times 10^{-3}$ m³/sec. This amounts to $\dfrac{2{\cdot}36 \times 10^{-3}}{0{\cdot}167} \times 100 = 1{\cdot}4\%$, and is close enough to the assumed value of 2 per cent that no corrections need be made.

Design of Vanes : As pointed out in Section 6.8, there are two methods of laying out the vane shape. The vanes will be designed by each of these methods in turn.

The radial components v_{r_1} and v_{r_2} of the absolute velocity at the inlet and outlet are 4 and 3·6 m/sec respectively. These are plotted against the corresponding radii of 9·5 cm and 17·7 cm, respectively, in Fig 6.10 and may be connected by a straight line or by a smooth curve, as shown. The vane angles β_1 and β_2 at the inlet and outlet are 13° and 20°. Since $w = \dfrac{v_r}{\sin \beta}$, the relative water velocities w will be $\dfrac{4}{\sin 13°} = 17{\cdot}8$ m/sec at the inlet, and the corners are rounded off as described in the previous section, with the aid of a planimeter to measure the areas.

The average velocity of the water leaving the volute is about 11·5 m/sec. According to Section 6.3 it would be desirable to have it leave the pump with a velocity of about 5·5 to 7·5 m/sec. A 20 cm-diameter flange has an area of 314 cm²; this corresponds to an average velocity of $\frac{0 \cdot 167}{0 \cdot 0314} = 5 \cdot 3$ m/sec which will be satisfactory. The section between the volute outlet and the discharge line, known as the discharge nozzle, would be made diverging to a 20 cm diameter.

Figure 6.18 shows sections of the volute passage at the calculated points with the areas increased approximately 10 per cent for

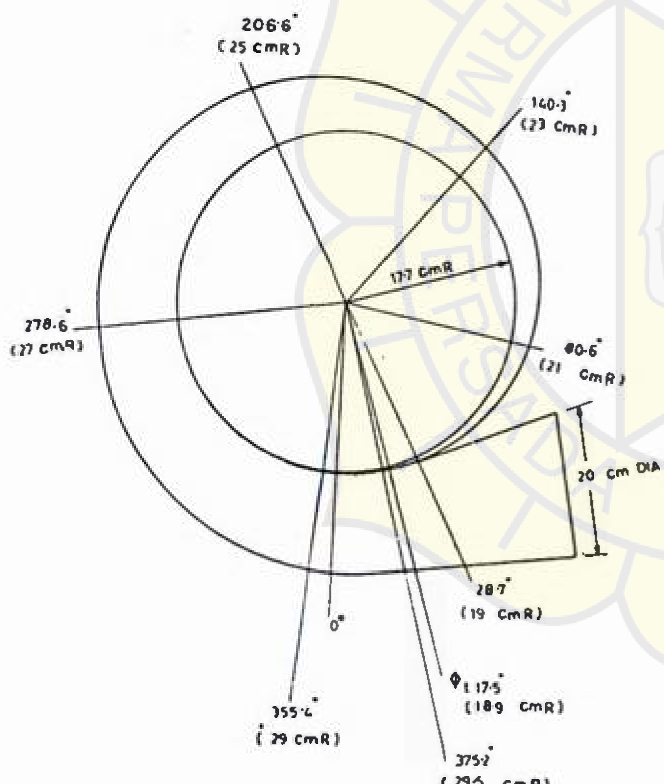

Fig 6.19 Elevation of volute.

values as calculated in the table.

6.12 Design of Diffuser—As outlined in Section 3.18 a diffuser has essentially the same shape as a volute except that a number of passages are used rather than one. This permits the conversion of kinetic energy to pressure in a much smaller space, so a diffuser is frequently used for stages having high heads, as in multistage pumps.

The radial clearance between the impeller and diffuser vane tips should be fairly small for good efficiency. It varies between 0·75 and 3 mm., depending upon the impeller size. The diffuser width b_3 may be made wider than the impeller outlet width. The water cannot follow this abrupt change; hence small pockets of inactive flow will be formed, as noted in the volute. For this reason the full throat area of the diffuser may not be effective.

The water travelling between the impeller and diffuser follows a logarithmic spiral of constant angle α'_2 as noted in Section 2.12 (*d*). Neglecting friction and turbulence, the velocity of the water at the diffuser throat will be $v_3 = v'_2 \frac{D_2}{D_3}$.

Each passage is assumed to handle equal fractions of the total flow. The total throat area required, A_3 is $\frac{Q}{v_3}$ and if z' is the number of vanes or passages, the throat height, h_3, is $\frac{A_3}{z' b_3}$.

The number of diffuser vanes z' should be a minimum consistent with good guidance of the water. In order to avoid vibration difficulties, the number of vanes should have no common factor with the number of impeller vanes. If possible the section of the passages in the diffuser is made nearly square, i.e., $b_3 = h_3$, since this will reduce the friction losses.

The shape of the passage should be diverging. Experiments indicate that this divergence angle should be between 10° and 12° for best results. If the velocity or viscosity of the liquid is high, the angle must be made smaller. General practice is to keep the angle small near the throat where the velocity is high and gradually increase it as the velocity decreases. The losses in the diffuser are rather high. The percentage of kinetic energy that is converted to pressure ranges from 75 to 90 per cent.

The velocity of the water leaving the diffuser is made slightly greater than the velocity in the discharge line from the pump.

The head produced at the hub is lower than that at the periphery; both are equalized in the casing beyond the impeller without cross flows, by conduction. It can be shown that the pump total integrated head H is the arithmetical average of the head generated at the hub and at the periphery and equal also to the head produced at the mean effective diameter. Point E on Fig. 11b is determined by the intersection of the line representing the discharge angle at the mean effective diameter (not shown on figure).

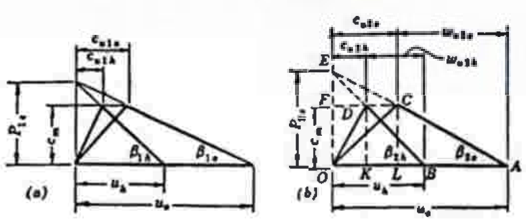

FIG. 11. (a) Axial flow pump entrance triangle with prerotation. (b) Discharge velocity triangle (Euler's), axial flow pump. (Stepanoff, *op. cit.*)

The ratio P_{2s}/c_{m2} (called the impelling ratio) is an important design factor and can be obtained from Fig. 25.

IMPELLER LAYOUT. The impeller profile is drawn for the known impeller eye and impeller outside diameter, and the meridional velocities at entrance and discharge. For the average range of specific speeds (1500 to 4500) three flow lines are sufficient, a_1a_2, b_1b_2, and c_1c_2 (Fig. 12a). The middle flow line can be drawn as a line dividing the flow into two equal parts or drawn as a median line between the two shroud profiles. The latter method is simpler and just as accurate as the first. Next, one of the flow lines (a_1a_2) is divided into a number of parts and then laid out the same distances along the remaining flow lines, points 1a, 2$a \cdots$ 8a; 1b, 2$b \cdots$ 10b; 1c, 2$c \cdots$ 11c. Parallel lines spaced g_1, g_2, $g_3 \cdots$ apart, equal to the spacing along the flow lines, are drawn on a plane for the vane development, Fig. 12b. The vane development of each flow line is drawn on this plane, using the vane angles β_1 and β_2, between the parallel lines limiting the flow lines on profile 1a, 8a; 1b, 9b; 1c, 10c. The true vane thicknesses s_u, s_{u1}, s_{u2}, etc., are drawn for each flow line (c_1c_2 is shown only on Fig. 12b). Now the flow lines are plotted on the plan view (Fig. 13a) point by point. The radial distances for each point are taken from the elevation view r_{1a}, $r_{2a} \cdots$ (Fig. 12a), while the advances of each point along the circles D_2, r_{1a}, $r_{2a} \cdots$ are h_1, h_2, $h_3 \cdots$ (from Fig. 12b). The construction of flow line a_1a_2 is shown; b_1b_2 and c_1c_2 are plotted in the same manner.

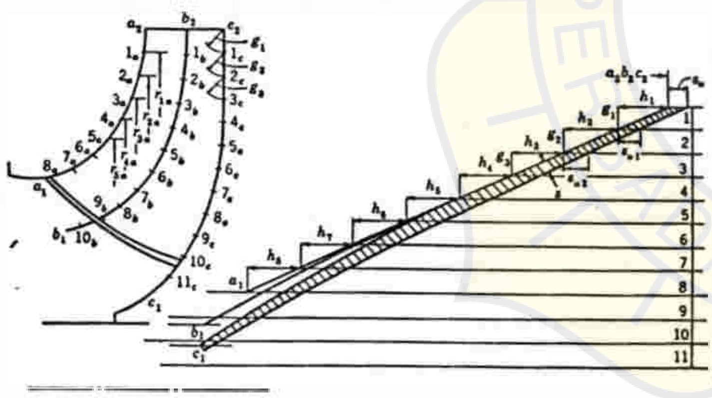

FIG. 12 (*a* and *b*). Mixed flow impeller profile and vane plane development. (*Stepanoff*, op. cit.)

The vane thickness s_u, s_{u1}, s_{u2}, etc., taken from the vane development, is laid off along the arcs of radii r_{1a}, r_{2a}, etc. The flow lines are the first set of construction lines used for plotting the vane pattern sections. For a second set of lines uniformly spaced radial sections are drawn on the plan view such as I, II, III (Fig. 14). The intersections of the flow lines it is better to separate the views of the front and back sides of the vane, showing them in their respective positions for two adjacent vanes. This will define the impeller channel and determine the shape of the core box if individual core boxes are made for each impeller channel. However, except for very large impellers, one core is made for the whole impeller. It is baked with metal vanes in place and then broken to remove the vanes, after which the parts of the core are reassembled. For a pattern of this type the wooden vane pattern is first made, from which metal vanes are cast.

of the board sections with the radial lines I, II, III for plotting. To avoid confusion of

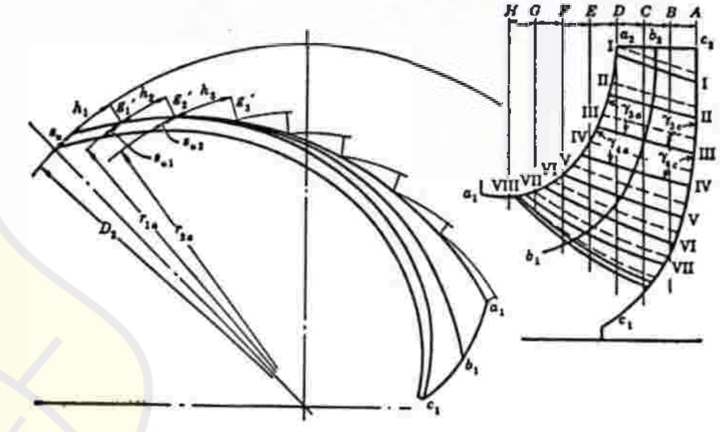

FIG. 13. (*a*) Impeller vane plan view; (*b*) Radial sections on profile view. (Stepanoff, *op. cit.*)

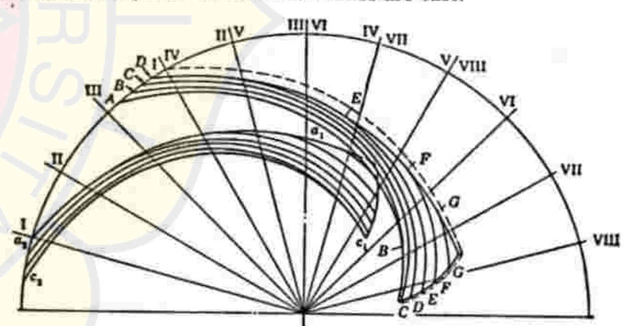

FIG. 14. Vane pattern sections. (Stepanoff, *op. cit.*)

To build the wooden vane, the vane sections are cut to proper shape and thickness and, when they are glued together in the proper order and their corners shaved off, they will give the vane shape. The vane section drawings are obtained by placing the two views of the front and back sides of the vane in their true relative position, one on top of the other. From this the vane sections can be picked out for each board.

Hydraulically, the best form of impeller channel is obtained when the true angles between the impeller vanes and shrouds are close to 90 degrees. For impellers having considerable curvature in their profiles, and for all extreme mixed-flow and axial-flow impellers, this becomes difficult to accomplish. The channel form may be improved by tilting the vane with respect to the shrouds. This is done by moving the flow lines on the plan view through a certain angle in respect to each other, thus changing the angle between the vane and the impeller shrouds without changing the vane angularity (compare Fig. 14 with Fig. 13a). The radial sections I, II $\cdots$ on the elevation view give approximately the

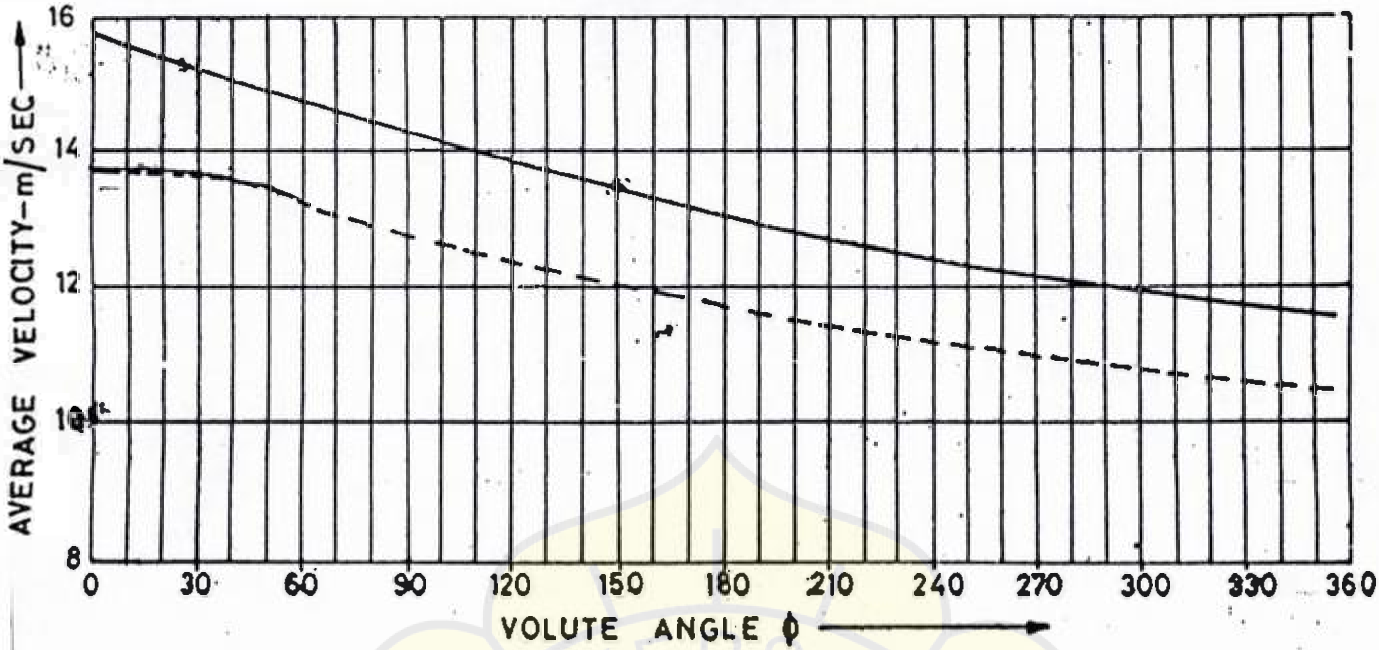
AVERAGE VELOCITY–m/SEC
16
14
12
10
8
0
30
60
90
120
150
180
210
240
270
300
330
360
VOLUTE ANGLE ϕ